SMAR 2015 – Third Conference on Smart Monitoring,
Assessment and Rehabilitation of Civil Structures

SMAR 2015

Properties of RC walls produced by infilling a frame with concrete for seismic rehabilitation

Dionysis Biskinis[1], Apostolos Psaros-Andriopoulos[1], and Michael N. Fardis[1]

[1]University of Patras, Greece

ABSTRACT: In seismic retrofitting of concrete buildings, frame bays are converted to reinforced concrete (RC) walls by infilling the space between the frame members with RC of a thickness of not more than their width. The cyclic behavior of the resulting wall depends on the connection between the RC infill and the surrounding RC members. The paper uses results from 48 cyclic tests of such composite walls to express their properties in terms of the geometry, the reinforcement and the connection. Properties addressed are: a) the yield moment at the story base; b) the secant-to-yield-point stiffness over the shear span of the wall in a story; c) the deflection at flexural failure in cyclic loading; d) the cyclic shear resistance, including sliding shear. Separate models are given for squat walls failing in shear. The models are modifications of the ones developed in the past for monolithic RC walls from several hundred cyclic tests.

1 INTRODUCTION

Adding RC walls to existing RC buildings is very popular and effective for seismic retrofitting. A simple and cost-effective way to add new walls is by infilling with RC some bays of the old frame, especially at the perimeter. A poor connection between the old members and the new parts of the wall may lead to reduced ductility or brittle failure of web panels. Moreover, if there is no integral connection between the existing and the new parts, the seismic behavior is uncertain and the wall may not be confidently modelled and checked as a single integral element. Several experiments have been conducted to date on one-bay RC frames converted to RC walls by adding a web between the frame members, not thicker than the surrounding beams or columns. The test results have not been used so far to develop rules for those properties of a RC-infilled frame which are needed in order to model it for the analysis and to check it on the basis of the analysis results: effective stiffness, moment and shear resistance, deformation at yielding and cyclic deformation capacity. The goal of this paper is to fill this gap.

2 CONNECTION OF THE NEW WEB TO THE SURROUNDING FRAME MEMBERS

Test results of 48 retrofitted specimens (and 13 monolithic companions) are used to develop rules for the estimation of the properties of interest. The specimens had up to three stories, but most had just one. Their low aspect ratio promotes shear-controlled cyclic behavior and failure. The small thickness of the RC infill compared to the width of the frame members is another common feature which penalizes shear resistance. The type and the details of the connection of the new web to the surrounding frame members have important ramifications for the cyclic behavior of the composite member and should be taken into account in the quantification of its properties: the closer to monolithic the connection, the better and simpler is the approximation

of these properties by extending/modifying the rules that apply to monolithic concrete walls. Various types of connection are used in the specimens considered here:

1. Monolithic wall (companion specimen, for comparison): 13 tests;
2. Connection of the new web only to the horizontal members via mechanical anchors: 2 tests;
3. As in 2, but to all surrounding frame members: 5 tests;
4. As in 3, but with epoxy-grouted anchors (in principle the most effective connection): 23 tests;
5. Bands of bars in the web (diagonal or parallel to the sides) welded to those of the surrounding frame members: 6 tests;
6. As in 4, combined with enlargement of the columns of the frame: 2 tests;
7. Without any connection: 2 tests;
8. An existing monolithic web is thickened without connection to the frame members: 1 test;
9. By means of shear keys: 2 tests;
10. A gap is left between the top of the new wall and the beam soffit: 5 tests.

Critical for the flexural behavior of the composite wall is the connection of the new web to the top of the underlying horizontal component of the frame (e.g., the top of a foundation beam at the base between the two columns, or of an intermediate story beam). Preferably, the vertical reinforcement of the new web should be fully anchored there, to develop its full tensile resistance. This is feasible in connection types 1 to 6, where short anchors of high tensile resistance cross the horizontal interface, with one end firmly secured to the existing horizontal member (chemically or mechanically) and the other protruding into the new web to collect the tensile forces of its vertical bars and to anchor them into the horizontal member.

3 PROPERTIES AT YIELDING – ULTIMATE CHORD ROTATION IN FLEXURE

It is presumed that the connection of the new RC infill to the frame members aims to achieve a cyclic behavior as close as possible to that of a monolithic wall. So, the rules for the properties of the composite wall are variations of those applying to monolithic walls, inferred from the tests analyzed in this study. Two sections are considered in each story of the composite wall:

1. The section at the base of the story, denoted and indexed by 0; if the starter bars crossing section 0 are fully anchored below, they act as the web vertical reinforcement of that section;
2. The section where the starter bars from below stop and only the web bars continue vertically (index: d); its distance from the base is the embedment length of starter bars in the infill, l_d.

As the acting moment of Section 0 is always larger than that of Section d, Section 0 cracks first; so, it controls the cracked stiffness of the wall story. However, as the starter bars serving as anchors normally have higher tensile strength per linear meter of the horizontal interface than the vertical reinforcement of the new web, Section d may have lower yield strength than Section 0 and, despite its lower acting moment, may yield first, controlling the wall's yield moment.

The yield stress of the web bars, denoted by $f_{yv,0}$ and $f_{yv,d}$ at sections 0 and d respectively, is in general different from that of the bars of the frame columns, $f_{y1} = f_{y2}$, which play the role of the tension and compression chords. Normally, all these bars are lap-spliced, starting at section 0. The effective stress in tension of a lap-spliced bar is its actual yield stress times $\min(1; l_o/l_{oy,min})$, where l_o is the actual lapping of the bar and $l_{oy,min}$ the minimum lapping required so that the lap splicing does not have an adverse effect on the yield moment of the section (Biskinis and Fardis 2010b, CEN 2005). The effective yield stress of the tension chord is the minimum of the two effective yield stresses: in the web, $f_{yv,eff}$, and in the tension chord itself, $f_{y1,eff}$. Column bars lap-spliced starting at section 0 count as double in compression (Biskinis and Fardis, 2010b, CEN 2005). With these considerations concerning lap-spliced bars, section analysis gives the yield

moment and the yield curvature of sections 0 and d, $M_{y,0}$, $\varphi_{y,0}$ and $M_{y,d}$, $\varphi_{y,d}$, respectively. The effective yield moment at the base of the story is either $M_{y,0}$, or the base moment at the instant Section d yields, whichever is smaller. If $L_{s,0}$ is the shear span (M/V ratio) at Section 0, then:

$$M_y = \min[M_{y,0};\ M_{y,d}(1+l_d/L_{s,0})] \quad (1)$$

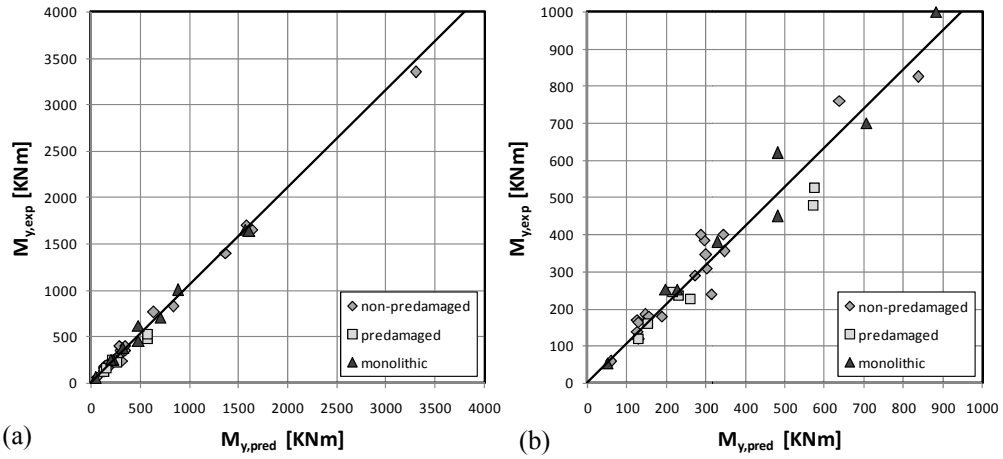

Fig. 1: Walls with flexural yielding: (a) experimental yield moment v prediction of Eq. (1); (b) detail.

Fig. 1 and rows 1 and 2 in Table 1 show that Eq. (1) agrees well with the results from tests of composite walls. Damage of the frame by cyclic testing before infilling it with RC and converting to a wall does not affect the agreement.

Section 0 cracks first and controls the cracked stiffness; the secant-to-yield-point stiffness of the wall story is:

$$EI_{eff} = M_{y,0}L_{s,0}/3\theta_{y,0} \quad (2)$$

where $\theta_{y,0}$ is the chord rotation at yielding of section 0 per Grammatikou et al (2015):

$$\theta_{y,0} = \phi_{y,0}\frac{L_{s0} + a_V z}{3} + 0.00075\left(1+\frac{h}{L_{s,0}}\right) + \frac{\phi_{y,0} d_b f_{y,eff}}{8\sqrt{f_c}} \qquad (f_y, f_c \text{ in MPa}) \quad (3)$$

In Eq. (3):

- $a_V z$ in the first term (reflecting flexure) is the tension shift of the moment diagram, with:
  - z = internal lever arm, equal to the center-to-center distance of the two old columns,
  - a_V=1 if diagonal cracking precedes flexural yielding of section 0 (ie, if $M_{y0}/L_{s0} > V_{Rc}$, with V_{Rc}: shear resistance of the composite wall without shear reinforcement; otherwise a_V=0;
- d_b is the diameter of the tension reinforcement and $f_{y,eff} = \min(f_{yl,eff}, f_{yv,eff})$ is the effective yield stress as defined above.
- the last term is the fixed-end-rotation due to slippage of the starter bars along their length below section 0; it is omitted, if these bars are epoxy-grouted into the frame member.

As the wall story yields when the moment at section 0 is the one from Eq. (1), which may be less than M_{y0}, the chord rotation at section 0 at apparent yielding of the wall, θ_y, may be less than θ_{y0} from Eq. (3). It is the value reached when the moment at the base becomes equal to M_y, from Eq. (1), and is attained with an effective stiffness of the story, EI_{eff}, from Eq. (2):

$$\theta_y = M_y L_{s,0}/3EI_{eff} \quad (4)$$

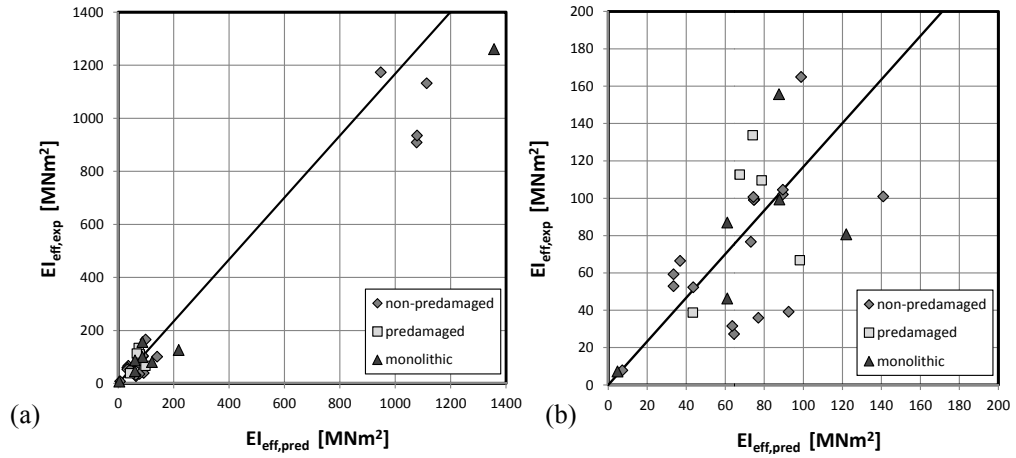

Fig. 2: (a) Test v prediction of Eq. (2) for secant-to-yield-point stiffness; (b) detail of (a).

As shown in Fig. 2 and in rows 3 and 4 of Table 1, Eq. (2) agrees well with the test results of composite walls. Damage of the frame by cyclic testing before infilling it with RC and converting it into a wall does not affect the agreement.

The few specimens which failed in flexure show that flexural failure of the wall story is controlled by the base section and takes place at a plastic ultimate chord rotation as given in Grammatikou et al (2015) for monolithic walls. Assuming that starter bars epoxy-grouted in the frame member do not slip there and neglecting the effect of lap-splicing of the web bars:

$$\theta_u^{pl} = \theta_u - \theta_y = a_{st}^{pl} a_{w,r} a_{w,nr} (0.25)^{\nu} \left(\frac{\max(0.01;\omega')}{\max(0.01;\omega)} \right)^{0.3} (f_c)^{0.2} \left(\min\left(9; \frac{L_s}{h}\right) \right)^{0.35} 25^{\left(\frac{a\rho_{sh} f_{yh}}{f_c}\right)} 1.275^{100\rho_d} \quad (5a)$$

$$\theta_u^{pl} = \theta_u - \theta_y = a_{st}^{hbw} \left(1 - 0.052 \max\left(1.5; \min\left(10; \frac{h}{b_w}\right)\right)\right) (0.2)^{\nu} \left(\frac{\max(0.01;\omega')}{\max(0.01;\omega)} \min\left(9; \frac{L_s}{h}\right) \right)^{\frac{1}{3}} (f_c)^{0.2} 25^{\left(\frac{a\rho_{sh} f_{yh}}{f_c}\right)} 1.225^{100\rho_d} \quad (5b)$$

with θ_y from Eq. (4), f_c raised to the power 0.2 in MPa and the other variables defined as:

a^{pl}_{st}=0.0143, a^{hbw}_{st}=0.017 for ductile steel and a^{pl}_{st}=0.0069, a^{hbw}_{st}=0.0073 for brittle steel;

$a_{w,r}$= 0.6 for rectangular walls, $a_{w,r}$=1 for non-rectangular ones (as well as for beams or columns, Biskinis and Fardis 2010a);

$a_{w,nr}$=0.77 for walls with non-rectangular section (T-, I-, H-, C-, as well as hollow rectangular) and $a_{w,nr}$=1 for rectangular section (including beams and columns, Biskinis and Fardis 2010a);

b_w: width of *one* web, even in cross-sections with two or more webs along the plane of bending;

$\nu = N/(bhf_c)$, with b the compression flange width and N the axial force (N> 0 for compression);

$\omega = (\rho f_{y1,0} + \rho_v f_{yv,0})/f_c$: total mechanical reinforcement ratio of tension and web longitudinal bars;

$\omega' = \rho' f_{y2,0}/f_c$: mechanical reinforcement ratio of compression bars at base section;

L_s/h: shear-span-to-depth ratio,

$f_{y1,0}$, $f_{yv,0}$: yield strength of the tension/compression and web longitudinal reinforcement at base;

ρ_d: steel ratio of bars at ±45° to the base section (if any) per direction;

$\rho_{sh}=A_{sh}/b_w s_h$: ratio of column confining steel parallel to the plane of bending; f_{yh}: its yield stress;

a: confinement effectiveness factor in the column:

$$a = \left(1 - 0.5 s_h / b_o\right)\left(1 - 0.5 s_h / h_o\right)\left(1 - \sum b_i^2 / (6 b_o h_o)\right) \quad (6)$$

where s_h is the centerline spacing of the ties in the column and b_o, h_o the dimensions of its confined core to the tie centerline, and b_i the on-center spacing along the column perimeter of the longitudinal bars (index: i) engaged by a tie corner or a cross-tie hook.

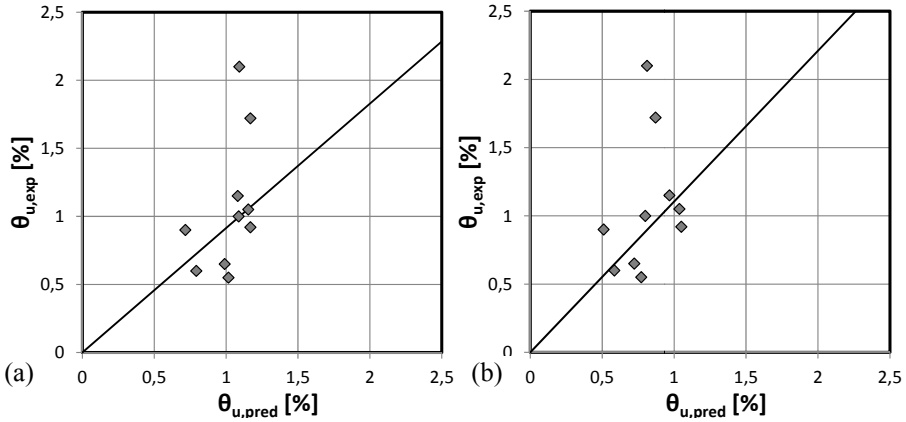

Fig. 3: Experimental ultimate chord rotation in cyclic flexure v prediction of (a) Eq. (5a); (b) Eq. (5b).

4 CYCLIC RESISTANCE OF WALLS FAILING IN SHEAR

4.1 Sliding shear failure of the composite wall at the section of flexural yielding

Most composite wall specimens failed by sliding along the section which controls flexural yielding. Grammatikou et al. (2015) fitted three alternative models to the sliding shear resistance of 55 monolithic walls under cyclic loading after flexural yielding. All three models are modifications of models in design codes: those in the ACI318 code and the *fib* Model Code 2010 (MC2010) for monotonic shear, as well as the cyclic model in Part 1 of Eurocode 8 for walls of Ductility Class High. Rows 9 to 14 of Table 1 list statistics of the experimental sliding shear resistance to the predictions from the three modified models. Fig. 4(a) compares the test results to the predictions of the two simpler ones among the models, which also give the best agreement to the present test results. The modified models are summarized below:

Modified ACI318 model:

$$V_{R,SLS,ACI,mod} = \left(1 - 0.02\mu_\theta^{pl}\right)\min\left(\sum\left[A_s f_y\left(\mu\sin\phi + \cos\phi\right)\right] + \mu N;\ \beta f_c A_c\right), \quad \beta = 0.1, \quad \mu = 0.625 \quad (7)$$

Modified *fib* MC2010 model:

$$V_{R,SLS,fib,mod} = \left(1 - 0.025\mu_\theta^{pl}\right)\cdot$$
$$\min\left(c_r f_c^{\frac{1}{3}} A_c + \kappa_1 \sum A_s f_y\left(\mu\sin\phi + \cos\phi\right) + \mu N + \kappa_2 \sum A_s \sqrt{f_c f_y}\,\sin\varphi;\ 0.5\beta_c \min\left(0.55; 0.55\left(\frac{30}{f_c}\right)^{\frac{1}{3}}\right) f_c A_c\right) \quad (8)$$

where f_c in the first and the last term of Eq. (8) is in MPa, and

$\mu_\theta^{pl}=\mu_\theta-1$: plastic chord rotation ductility factor, with $\mu_\theta=\theta/\theta_{y0}$ and θ_{y0} from Eq. (3),

the sums extend over all bars crossing (at an angle φ to the horizontal) the section predicted by Eq. (1) to control the yield moment at the base of the composite wall,

A_c: gross area of the section,

Eq. (8) uses the monotonic values per *fib* MC2010 for smooth interfaces: $c_r=0$, $\mu=0.6$, $\beta_c=0.4$, $\kappa_1=0.5$, $\kappa_2=1.1$.

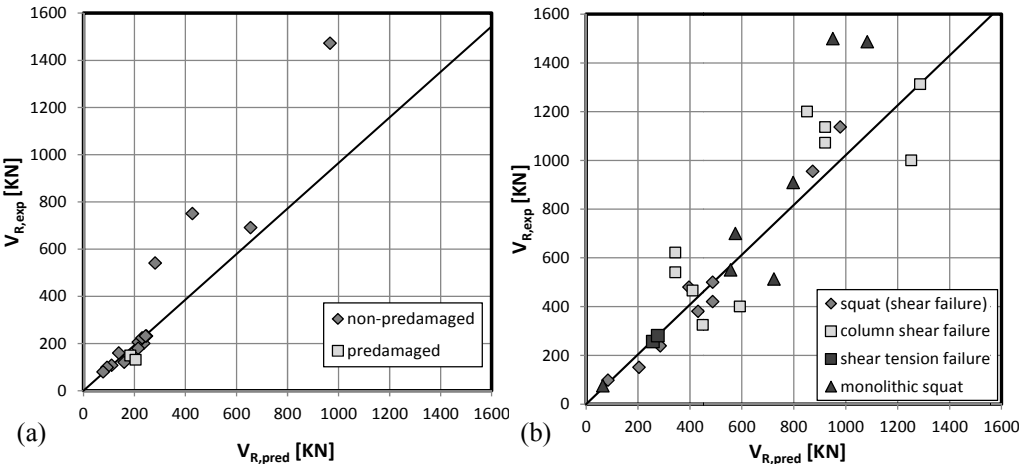

Fig. 4: Experimental v predicted shear strength: (a) in sliding shear (indicatively for Eq.(8), modified *fib* MC2010); (b) of squat walls per empirical Eq.(11) or in shear tension or due to column shear failure.

4.2 Cyclic shear resistance of squat walls ($L_s/h \le 1.2$)

Grammatikou et al. (2015) fitted two models to 320 tests of monolithic squat walls (with $L_s/h\le 1.2$). The first one is a physical model, applies for $0.25\le L_s/h\le 1.2$, and gives the shear resistance, $V_{R,squat}$, as the sum of a contribution of concrete, V_c, and a contribution of the web bars, V_s:

$$V_s=\min\left\{\begin{array}{c}\rho_h b_w \min\left((d-x)/\tan\theta_{cr}, L_s\right) f_{yh} \\ \left(\rho_v b_w \min\left(L_s\tan\theta_{cr}, d-x\right) f_{yw}+A_s f_y\right)/\tan\theta_{cr}\end{array}\right\} \quad (9a)$$

$$V_c=\left(1+150\rho\right)\left(1-0.725\frac{L_s}{h}\right)\left(\frac{2}{3}A_c f_{ct}\sqrt{1+\frac{N}{A_c f_{ct}}}\right) \quad (9b)$$

where:

$\rho_h=A_{sh}/b_w s_h$, $\rho_v=A_{sv}/b_w s_v$: ratios of horizontal and vertical web reinforcement, respectively,

ρ: tension reinforcement ratio.

f_{ct}: concrete tensile strength, calculated here as $f_{ct}=0.3f_c^{2/3}$ per *fib* MC2010,

θ_{cr}: angle of diagonal crack to the vertical, which does not always cross the full section depth:

$$\theta_{cr}(^o)=60^o-15L_s/h\ge 45^o \quad (10)$$

The second model is empirical (a modification of one fitted in Gulec and Whittaker (2011) to the peak resistance of a smaller sample of monolithic squat walls) and applies for $0<L_s/h\le 1.2$:

Rectangular walls:

$$V_{R,squat,2} = \frac{0.035A_{c,eff}f_c + 0.32A_{sv}f_{yv} + 0.18A_{sh}f_{yh} + 0.17A_sf_y + 0.2N}{\sqrt{L_s/h}} \le 1.3\sqrt{f_c}A_{c,eff} \quad (11a)$$

Non-rectangular or barbelled walls:

$$V_{R,squat,2} = \frac{0.04A_{c,eff}f_c + 0.225A_{sv}f_{yv} + 0.1A_{sh}f_{yh} + 0.3A_sf_y + 0.25N}{\sqrt{L_s/h}} \le 1.3\sqrt{f_c}A_{c,eff} \quad (11b)$$

where, A_s is the tension reinforcement area and $A_{c,eff}$ − as in Gulec and Whittaker (2011) − is the cross-sectional area of the web, increased by the area of the flanges up to a distance from the web mid-plane of one-half the wall shear span, L_s.

Table 1: Statistics of test-to-prediction ratio of yield properties, ultimate chord rotation and shear strength

Test-to-prediction ratio	# tests	sample statistics [1] mean	median	CoV %
1. $M_{y,exp}/M_{y,Eq.(1)}$ RC-infilled frames with flexural yielding in the test [2]	32	1.09	1.055	16.0%
2. $M_{y,exp}/M_{y,pred}$ monolithic companions with flexural yielding	11	1.10	1.085	9.9%
3. $EI_{exp}/EI_{pred,Eq.(2)}$ RC-infilled frames with flexural yielding in the test [2]	29	1.16	1.16	37.2%
4. $EI_{exp}/EI_{pred,Eq.(2)}$ monolithic companions with flexural yielding in the test	8	1.095	1.03	40.0%
5. $\theta_{y,exp}/\theta_{y,Eq.(4)}$ RC-infilled frames with flexural yielding in the test	29	1.10	0.925	44.4%
6. $\theta_{y,exp}/\theta_{y,Eq.(4)}$ monolithic companions with flexural yielding in the test	8	1.10	1.05	39.0%
7. $\theta_{u,exp}/\theta_{u,Eq.(5a)}$ RC-infilled frames with flexural failure in the test	10	1.025	0.915	40.8%
8. $\theta_{u,exp}/\theta_{u,Eq.(5b)}$ RC-infilled frames with flexural failure in the test	10	1.325	1.105	44.7%
9. $V_{R,exp}/V_{R,Eq.(7)}$ RC-infilled frames with shear sliding - modified ACI318 [2]	17	1.05	0.995	26.6%
10. $V_{R,exp}/V_{R,Eq.(7)}$ monolithic companions in shear sliding - modified ACI318	5	1.13	1.12	34.9%
11. $V_{R,exp}/V_{R,Eq.(8)}$ RC-infilled frames in shear sliding- modified *fib* MC2010 [2]	17	1.07	0.97	32.5%
12. $V_{R,exp}/V_{R,Eq.(8)}$ monolithic companions in shear sliding- mod. *fib* MC2010	5	1.095	1.015	38.8%
13. $V_{R,exp}/V_{R,mod.EC8}$ RC-infilled frames with shear sliding - modified EC8 [2]	17	1.35	1.28	38.9%
14. $V_{R,exp}/V_{R,mod.EC8}$ monolithic companions with shear sliding- modified EC8	5	1.11	1.075	26.3%
15. $V_{R,exp}/V_{R,Eq.(9)}$ squat RC-infilled frames ($0.25<L_s/h<1.2$), physical model	9	0.97	1.04	25.1%
16. $V_{R,exp}/V_{R,Eq.(9)}$ monolithic companions, physical model	7	1.19	1.14	22.2%
17. $V_{R,exp}/V_{R,Eq.(11)}$ squat RC-infilled frames ($L_s/h<1.2$), empirical model	9	1.00	1.025	17.1%
18. $V_{R,exp}/V_{R,Eq.(11)}$ monolithic companions, empirical model	7	1.165	1.155	23.7%
19. $V_{R,exp}/V_{R,Eq.(12)}$ diagonal tension failure after flexural yielding	2	1.005	1.005	1.3%
20. $V_{R,exp}/V_{R,Eq.(13)}$ column diagonal tension failure	10	1.15	1.15	32.1%

[1]: the median of a ratio is a more meaningful measure of its central tendency than the mean value
[2]: the additional flexural reinforcement in 6 specimens with type 5 connection is unknown and neglected: their M_y, EI_{eff} and sliding shear resistance are underestimated, increasing their mean, median and CoV.

4.3 Cyclic resistance of walls with Ls/h≥1.0 in diagonal tension after flexural yielding

Two wall specimens failed in diagonal tension after flexural yielding, a failure mode for which the cyclic shear resistance is (Biskinis et al, 2004, CEN 2005):

$$V_{R,ST} = \frac{h-x}{2L_s}\min\left(N;0.55A_cf_c\right) + \\ + \left(1-0.05\min\left(5;\mu_\theta^{pl}\right)\right)\left[0.16\max(0.5;100\rho_{tot})\left(1-0.16\min\left(5;\frac{L_s}{h}\right)\right)\sqrt{f_c}b_wd + V_s\right] \quad (12)$$

where the new variables are:

x: neutral axis depth at yielding – computed from section analysis alongside M_y, φ_y,

ρ_{tot}: total longitudinal reinforcement ratio,

d: effective depth of the section,

$V_s=\rho_h b_w z f_{yh}$: shear resistance due to the horizontal web reinforcement with $z=0.8h$ in rectangular walls, $z=d-d_s$ in non-rectangular ones (: distance between tension and compression chords).

Five specimens had a gap between the top of the web and the beam soffit, leading to a premature shear failure of the column tops. Five more specimens demonstrated a diagonal tension failure at the columns. For the above – 10 in total – specimens, their shear force resistance is calculated here as the sum from three separate diagonal tension shear resistance mechanisms, at the web and the two columns:

$$V_{R,tot}=V_{R,web,ST}+V_{R,col1,ST}+V_{R,col2,ST} \quad (13)$$

where Eq.(12) is used in all three terms, with the column under tension considered to have zero concrete contribution to shear strength (i.e., only the V_s term in $V_{R,col1,ST}$). The contribution of the axial force, i.e. the first term in Eq. (12), is taken as in the full composite wall. The last row of Table 1 gives the test-to-prediction statistics of Eq. (13) for these tests.

5 CONCLUSIONS

Models are proposed for the yield moment, the secant-stiffness-to-yield-point, the cyclic ultimate chord rotation and the shear resistance (due to diagonal tension, shear sliding and squat-wall effects) of the composite wall produced by infilling with RC the space between two RC columns, without encapsulating them. They take into account the type and the detailing of the connection with the surrounding frame members and are rational, natural and simple modifications of models applying to monolithic walls; they allow to model the composite wall in analysis and to verify it in flexure or shear as an equivalent monolithic wall.

ACKNOWLEDGEMENT

The research leading to these results receives funding from the General Secretariat for Research and Technology under grant ERC-12 of the Operational Program "Education and lifelong learning", co-funded by the European Union (European Social Fund) and national resources.

REFERENCES

Biskinis D, and Fardis MN, 2010a, Flexure-controlled ultimate deformations of members with continuous or lap-spliced bars. *Structural Concrete* 11 (2) 93-108

Biskinis D, and Fardis MN, 2010b, Deformations at flexural yielding of members with continuous or lap-spliced bars. *Structural Concrete* 11 (3) 127-138

Biskinis D, Roupakias G. and Fardis MN, 2004, Degradation of shear strength of RC members with inelastic cyclic displacements. *ACI Structural J.* 101(6) 773-783

CEN, 2005, EN1998-3:2005 *Eurocode 8: Design of structures for earthquake resistance. Part 3: Assessment and retrofitting of buildings* Comite Europeen de Normalisation. Brussels

Grammatikou S, Biskinis D, and Fardis MN, 2015, Strength, deformation capacity and failure modes of RC walls under cyclic loading. *Bulletin of Earthquake Engineering*, Online April 24, 2015, DOI 10.1007/s10518-015-9762-x..

Gulec CK, Whittaker AS, 2011, Empirical equations for peak shear strength of low aspect ratio reinforced concrete walls *ACI Structural J* 108(1): 80-89.